GEOPHYSICAL RESEARCH LETTERS, VOL. 28, NO. 24, PAGES 4521-4524, DECEMBER 15, 2001

Plasma Density Distribution Along the Magnetospheric Field: RPI Observations From IMAGE

B.W. Reinisch[1], X. Huang[1], P. Song[1], G. S. Sales[1], S. F. Fung[2], J. L. Green[2], D. L. Gallagher[3], and V. M. Vasyliunas[4]

Abstract. A new technique is introduced that remotely measures the plasma density profile in the plasmasphere. Radio plasma imager (RPI) echo observations provide echo delay time as function of frequency, from which the plasma density as function of position along the magnetic field line can be calculated. An example from the nightside plasmasphere (L=3) shows the density having its minimum value near the equator and rapidly increasing densities along the field line above 40° magnetic latitude. The density increases at a faster rate toward the ionosphere than the field strength. The index of the power law of the density as a function of field strength increases from a few tenths near the equator to close to unity near 40° and greater than 2 near the ionosphere.

1. Introduction

The global distribution of the plasma density is one of the most important pieces of information for space physics. It determines the distribution of charged matter and key physical parameters, such as the electron plasma frequency and Alfvén velocity, and hence the eigenfrequency of a field line. Furthermore, from the density distribution, some of the underlying physical processes can be inferred.

The plasma density distribution along the magnetic field has long attracted much interest because it is a test-bed for theoretical models involving different physical processes. Temporal changes in plasmaspheric density profiles further provide important information about the plasma loss and refilling processes of the magnetospheric dynamics. There are various models of how the density varies along the field line. A diffusion model predicts that in equilibrium the plasma density (N_e) along a flux tube is proportional to B [Newberry et al., 1989] as the cross-section of a flux tube is proportional to 1/B, where B is the strength of the magnetic field. Based on physical arguments, other models assume, however, that the density is proportional to B^2 [e.g., Khazanov et al., 1984]. Some empirical models suggest that the density remains the same at least in a large range of latitudes from the equator [Gallagher et al., 2000]. Therefore, an instantaneous measurement of the density along the field line is critical to understand the processes that determine the distribution of the plasma along a flux tube.

Conventional space measurements of N_e are made in-situ on space-borne platforms. These measurements provide N_e at each location along the satellite trajectory at different times. To interpret a measured density time series as N_e distribution along the trajectory, one assumes that the plasma is static, an assumption that is often not valid in many regions in space because plasma structures may move rapidly. Furthermore, many of the plasma detectors cover only a limited energy range. In many cases, a significant portion of the plasma at the lowest energies cannot be measured. At the lowest energies, the spacecraft electric potential has an important effect on the total measured intensity. Measuring N_e accurately by in-situ particle detectors is thus not trivial [e.g., Song and Russell, 1999].

The density can also be derived from the changes in the characteristics of the waves near the plasma frequency or upper hybrid frequency. This method has been confirmed by comparison with other density measurement methods [e.g., Carpenter et al., 1981; Song et al., 1993].

Global density distributions have been derived statistically [e.g., see a recent review by Lemaire and Gringauz, 1998]. These distributions can be binned according to solar wind or geomagnetic parameters to derive the average profile under each condition [e.g., Persoon et al., 1983; Carpenter and Anderson, 1992; Gallagher et al., 2000]. It is difficult in these models to determine the latitudinal dependence of N_e, i.e., the variation of N_e along the field line. To determine the field-aligned distribution requires many different trajectories along which the satellite measures different portions of the same flux tube, unless the trajectory is along the field for a significant portion of a flux tube. The space plasma conditions, however, may change significantly as the trajectory evolves.

2. RPI Remote Measurement Technique

The radio plasma imager (RPI) [Reinisch et al., 2000] on IMAGE [Burch et al., 2001] applies the radio sounding technique to measure N_e remotely. The RPI transmits coded signals from 3 kHz to 3 MHz in all directions and measures the echo delay time as a function of frequency. Echoes that experience the same dispersion in the propagation form a distinct trace in the "plasmagram", a display of signal amplitude as functions of frequency and echo delay time. The RPI uses three orthogonal thin-wire dipole antennas: two dipoles in the spin plane, nominally 500 meters long tip-to-tip, and one along the spin axis, 20 meters long. The spin period of the satellite is near 2 min. Passive measurements, similar to those of conventional plasma wave instruments, alternate with the active experiments discussed above. In the experiment discussed in this letter, the RPI transmitted a pulse and listened to the echoes, then sent a second pulse for improved signal-to-noise ratios. This process was repeated at each of 114 frequencies that were logarithmically spaced from 18 kHz to 1.5 MHz. A complete measurement was made in slightly over 2 min. The time resolution for the echo delay time was 3.2 ms (given by the pulse width) translating to a

[1]Environmental, Earth, and Atmospheric Sciences Department, Center for Atmospheric Research, University of Massachusetts Lowell
[2]NASA Goddard Space Flight Center, Greenbelt, MD
[3]NASA Marshall Space Flight Center, Huntsville, AL
[4]Max-Planck-Institut für Aeronomie, 37191 Katlenburg-Lindau, Germany

Paper number 2001GL013684.
0094-8276/01/2001GL013684$05.00

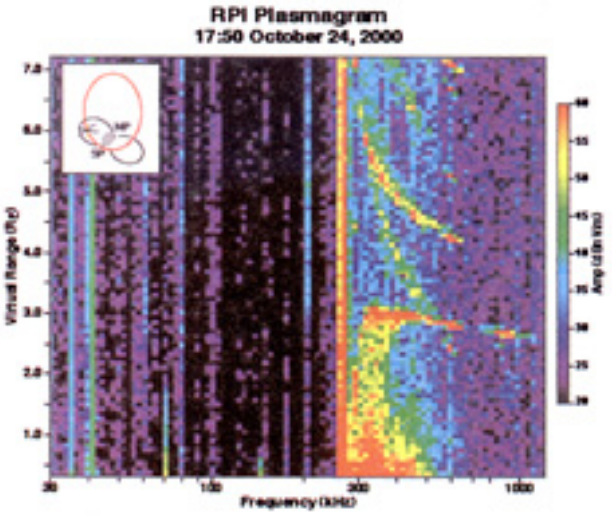

Figure 1. Plasmagram at 0733 UT, June 13, 2000, showing color-coded signal amplitude in dB as function of frequency and virtual range. The virtual range is the time delay of an echo multiplied by one half the speed of light *c*. The insert shows the orbit (red), locations of IMAGE (x), and the L=4 shells (black); NP and SP indicate the geographic poles.

spatial resolution of ~500 km if the signals travel at the free-space speed of light *c*.

When a wave propagates in the direction of increasing density, the wave is reflected at places where the wave frequency equals the cutoff frequency of the wave mode. The cutoff frequency of a given mode is a function of N_e, B, and propagation angle θ (angle between **B** and the wave normal). In the cold plasma theory there are three modes, referred to as X, O, and Z modes [Budden, 1988].

Although the RPI radio sounding, in principle, can receive echoes from all directions, we were surprised to observe that the most distinct echoes arrive in the magnetic field direction, suggesting wave propagation along the magnetic field lines. When IMAGE is in the polar region where the field line is nearly radial from the earth, the N_e profile in altitude can be derived and has been reported [Reinisch et al., 2001]. When IMAGE is in the equatorial region, field-aligned N_e profiles for both hemispheres can be derived. In this letter, we report and verify the results for one observational period when IMAGE was in the equatorial region.

On Oct. 24, 2000, at 1750 UT, IMAGE was at 22.8 MLT, –11.2° MLAT, and L=3. The invariant latitude is 55.2°. Figure 1 shows the plasmagram displaying the signal amplitude as a function of frequency and of time delay multiplied by *c/2* and presented as the so-called virtual range. The most striking echo traces are the two at middle and long ranges between 300 and 600 kHz. The wave normal direction of the arriving signals can be determined from the amplitudes and phases measured at the three antennas [Reinisch et al., 1999]. The measurements of these two traces, which will be referred to as the primary traces, show that the echoes are arriving along the model magnetic field line through the spacecraft location. The vertical lines near 35, 70, and 140 kHz in Figure 1 result from echoes and resonances of the local electron cyclotron harmonics [Benson, 1977; and references therein], consistent with the local electron gyrofrequency of 34.95 kHz predicted from a magnetic field model [Tsyganenko and Stern, 1996].

3. Inversion of Plasmagrams to Plasma Density Profiles

Plasma density inversion techniques from echo traces have been developed in radio science and applied to ionospheric physics [e.g., Jackson et al., 1980; Huang and Reinisch, 1982]. They are based on the theory of radio wave propagation in a cold plasma. Given the plasma density and field measured immediately next to the satellite and assuming a mode and a propagation direction relative to the magnetic field, the group velocity of the wave can, in principle, be determined from the dispersion relations. The group velocity and the time delay of the echo then determine the distance to the reflection point. The plasma density there can be determined from the reflection condition for the chosen mode, with the use of a global magnetic field model. This procedure can be continuously applied to points further away from the satellite, i.e. with echoes at increasingly higher frequency, and hence the density-distance profile can be derived. In practice, our inversion performs a best fit to an observed echo trace.

Two assumptions are needed: the mode and the propagation angle. For a given echo trace, one may try the three possible dispersion relations [Budden, 1988], and also look at possible mode coupling mechanisms. There are two possible outcomes for each try. First, using the selected mode does not yield a profile, implying that the chosen mode cannot propagate in the given direction and is a wrong choice. Second, the calculation does provide a density-location profile that reproduces the trace. This profile is then used to calculate the expected echo traces for other modes. If the calculated traces match the observations, it is likely that the profile is correct. This procedure is able to determine the real density profile that reproduces the observations without inconsistencies. For the inversion, two initial values -- N_e and B at the satellite location -- are needed. The density near the satellite is measured in-situ by the resonance at the plasma frequency or by the extrapolation of the echo trace. The global magnetic field is determined from an empirical model [Tsyganenko and Stern, 1996] and checked by the in-situ gyro resonance measurements as discussed above.

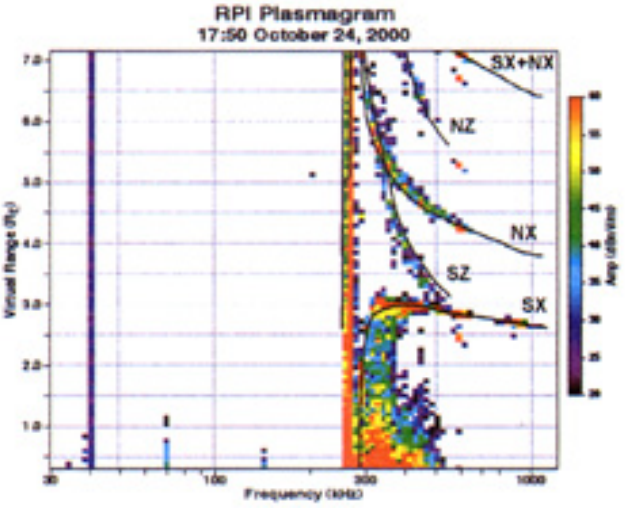

Figure 2. Reconstruction of the echo traces, black lines, using the inverted densities. The color code enhances observed traces in Figure 1. Labels S, N, X, and Z denote southern and northern hemispheres and X and O-Z-O traces, respectively. The NX trace has been extrapolated to higher frequencies.

To invert the plasmagram to N_e profiles, we first digitize the two primary echo traces (Figure 1), obtaining the echo time delay for each frequency. With the plasmagram's frequency resolution of 4% and the virtual range resolution of ~500 km, the uncertainty in the digitization does not result in any appreciable difference in the density inversion, in particular when the density change is more than 200~300%. The echo traces, global magnetic field model, and initial density are then input into the inversion program to test for various possible modes and possible propagation angles. Since the measurements indicate a wave normal direction approximately parallel to the field, we tested for θ between 0 and 10°. When θ increases beyond 5°, the recalculated traces become less consistent with the observation, in other words, smaller propagation angles give better predictions. The following results were derived with a propagation angle of θ = 0.5° parallel/anti-parallel to the magnetic field. The recalculated traces in Figure 2 confirm that the two primary traces, labeled SX and NX, are field-aligned X modes. No noticeably different X traces resulted for θ = 0°. The NX trace consists of X echoes from the northern hemisphere, and the SX trace of X echoes from the southern hemisphere. This is consistent with a picture in which N_e is approximately symmetric about its lowest value at the equator and the fact that IMAGE was below the equator.

Using the N_e profile that enabled the successful reconstruction of the primary traces, SX and NX in Figure 2, we assume θ = 0.5° and calculate the O-Z-O traces, labeled SZ and NZ. The O-Z-O traces are formed by waves that undergo two mode conversions. O mode waves transmitted from the satellite become Z mode waves before reaching the reflection points. On the way back to the satellite, they convert back to O mode waves. The same traces are commonly observed in ground-based and topside ionospheric sounding [Budden, 1988]. Although mode coupling is efficient for small θ, we expect the O-Z-O traces to be weaker than the X traces. The calculated SZ and NZ traces in Figure 2 match the observed weak-amplitude traces very well, confirming that the N_e profile and θ are correct. The weak-amplitude traces could not be reproduced by assuming an O mode wave with θ = 0° (L wave). The observed Z amplitudes are ~11 dB smaller than the X amplitudes, translating to a mode coupling efficiency of ~1/3. Furthermore, the partial trace at the largest virtual distances near 600 kHz, labeled SX+NX, is reproduced by assuming X mode waves that bounce at both hemispheres before being received by the RPI. The vertical enhanced line near 270 kHz is caused by the local plasma frequency oscillation. The more diffused echoes between 400 and 500 kHz and between 0.3 and 1.4 Re are those radially reflected from the lower plasmasphere/ionosphere, revealing irregularities in the inner plasmasphere.

Figure 3 shows the calculated N_e distribution along the field as functions of (a) the magnetic latitude, and (b) the strength of the magnetic field. Since the measurements of the echo traces were made in about 20 s, the N_e profiles can, for most purposes, be considered as being obtained instantaneously. The satellite traveled only about 100 km in that time. Therefore the measured profile represents the flux tube with a radius of less than 50 km near the equator.

The profile in Figure 3 is generally consistent with the statistical observational results at low and mid latitudes [Figure 7 of Gallagher et al., 2000]. The density increases relatively slowly near the equator and much faster at higher latitudes. If we describe the density variation locally as a power-law dependence,

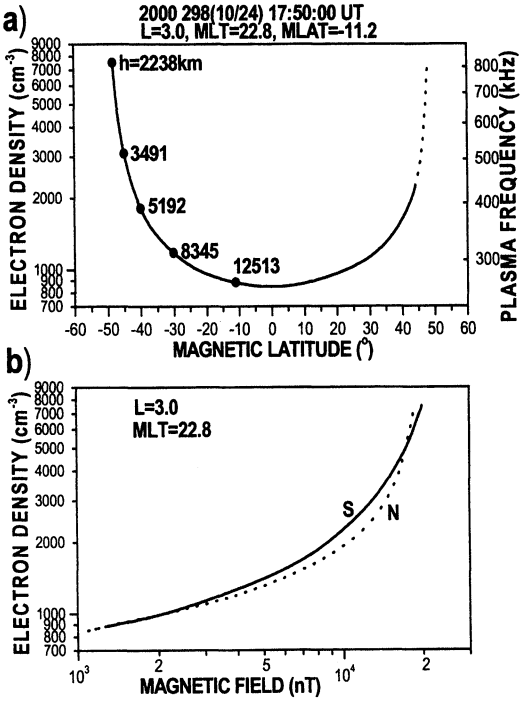

Figure 3. Density distribution along the field line (a) as function of magnetic latitude with altitude marked, and (b) as function of the strength of the magnetic field. The dashed-line segment in (a) is based on extrapolation of the NX trace. The solid (dashed) line in (b) is for the southern (northern) hemisphere.

$N_e \propto B^K$, then near the equator the density is proportional to only $B^{1/4}$. As the latitude increases, the density begins to increase more rapidly, until it increases faster than B^2 at the highest latitudes, having passed the slope characteristic of diffusive equilibrium models, N_e proportional to B, at about 40° latitude in the middle range of Figure 3b.

It may be premature to discuss the physical insights on global processes to be learned from this single event in particular because the density profile is expected to depend on the loss-refilling processes, which are functions of time relative to storm/substorm events. From a simple intuitive point of view, the plasmaspheric flux tubes are primarily filled locally from the ionosphere and emptied by the global magnetospheric convection flow that carries them to the outer magnetosphere. The quantity $V \cdot N_e/B$, where V is the field-aligned bulk velocity, is constant along a flux tube in the steady state and in the absence of local sources or sinks of plasma in the plasmasphere; it decreases (increases) in the direction of V where the density increases (decreases) with time or where sinks (sources) are present. V is expected to be in the direction from the ionosphere toward the equator, starting from near zero, accelerating to some (possibly quasi-constant) value, and then diminishing (in the absence of interhemispheric flow) to near zero again at the equator. The major features of the observed density profile can thus be explained by variations of V. The rather flat profile near the equator (increase of N_e/B as the equator is approached) follows from the expected decrease of V and the increase in density as the flux tube is filled. Wherever V is approximately constant, N_e is proportional to B. The rapid decrease of the density as one goes away from the ionosphere may reflect acceleration of the field-aligned flow, although undoubtedly there are many additional complications associated with the source and diffusion processes. It may be noted that the

earthward (anti-earthward) motion of the flux tube near the equator, which decreases (increases) the volume of the flux tube, tends to flatten (steepen) the profile if the density in the ionosphere remains the same.

4. Discussion

The most important result of our analysis is that the echoes are caused by field-aligned propagation. An interesting question is whether the waves, which are arriving at the satellite along the field line also propagated along the field in the more distant region where the field turns toward the ionosphere at high latitudes. There is no conclusive answer to this question unless there are simultaneous in-situ measurements along the field to independently verify the results. However, there is ample evidence that suggests our analysis to be correct. First of all, the high density we observe, of the order of 10^4 cm^{-3}, exists only near the ionosphere and not in the magnetosphere or solar wind. This eliminates the possibility that the signals propagate merely in north-south directions but not turn earthward when the field does. Second, there are two apparently separate X traces. Unless both of the X mode signals propagate along the field, it is not clear how other mechanisms can produce the two (not one and not more than two) primary traces with reasonable physical explanations. Third, the inversion method not only calculates the densities but also predicts the O-Z-O traces that are consistent with the observations. The O and Z modes and hence O-Z-O trace have different dependences on the magnetic field strength than the X mode, especially near the ionosphere where the field is stronger. Fourth, the SX+NX trace can be used as evidence for conjugate reflections on the same field line.

What causes the field-aligned propagation? There are two possibilities. First, the gradient of the refraction index is along the field and the electromagnetic waves propagating along the field will return to the spacecraft after reflection at cutoff. Waves at large angles will not be reflected back to the satellite. This mechanism does not require irregularities across the flux tube. It would predict the echo amplitude to be inversely proportional to the path length. The path length ratio of the NX and SX echoes in Figure 2 is ~1.5 to 2. The median measured amplitude difference is ~5 dB, corresponding to an amplitude ratio of 1.8. This measurement supports the above mechanism. Near the ionosphere the density gradient deviates from the field direction and the field line is no longer normal to the ionospheric plasma stratification. This could explain the abrupt termination of the X traces at ~600 kHz. However, how such a profile of the refraction index is formed and maintained remains unknown. Second, an alternate mechanism that can explain field-aligned propagation echoes is the existence of density ducts. The change in the index of refraction at the surface of the duct confines the wave propagation. The waves become trapped and bounce back in the duct. For a classical duct we expect the amplitudes of multiple echo traces to remain constant and not vary with path length, inconsistent with our observations. Further amplitude and ray tracing studies are required to determine the applicability and properties of any propagation model.

5. Conclusions

We have derived the plasma density along the magnetic field from one hemisphere to the other in one example of IMAGE-RPI radio sounding measurements. This profile, based on cold plasma theory, can reproduce 5 different echo traces observed in 20 s, leaving little possibility for alternative interpretations. In this example, the density is relatively flat near the equator and increases rapidly at high latitudes, consistent with a quasi-static equilibrium at low latitudes and active plasma transport from the ionosphere through the high-latitude plasmasphere. A database consisting of a large number of field-aligned traces is now available for construction of the density distribution in the plasmasphere under various geomagnetic conditions.

Acknowledgments. We thank D. L. Carpenter, R. F. Benson, and M. Liemohn, for helpful discussions. I. A. Galkin and G. Khmyrov provided Binbrowser analysis support. The work at UML was supported by NASA under subcontracts from Southwest Research Institute and by NSF under Awards NSF-ATM9729775 and NSF-ATM0077655.

References

Benson, R. F., Stimulated plasma waves in the ionosphere, *Radio Sci., 12,* 861, 1977.

Budden, K. G., *The propagation of Radio Waves,* 669 pp., Cambridge Univ. Press, New York, 1988.

Burch, J.L. et al., Views of Earth's magnetosphere with the IMAGE satellite, *Science, 291*, 541, 2001.

Carpenter, D. L., and R. R. Anderson, An ISEE/whistler model of equatorial electron density in the magnetosphere, *J. Geophys. Res., 97,* 1097, 1992.

Carpenter, D. L., R. R. Anderson, T. F. Bell, and T. R. Miller, A comparison of equatorial electron density measured by whistler and by satellite radio techniques, *Geophys. Res. Lett., 8,* 1107, 1981.

Galkin, I., G. Khmyrov, A. Kozlov, B. Reinisch, X. Huang, and G. Sales, New tools for analysis of space-borne sounding data, in *Proc. 2001 USNC/URSI National Radio Science Meeting, July 8-13, 2001,* 304, 2001.

Gallagher, D.L., P. D. Craven, and R. H. Comfort, Global core plasma model, *J. Geophys. Res., 105,* 18,819, 2000.

Huang, X. and B. W. Reinisch, Automatic calculation of electron density profiles from digital ionograms. 2. True height inversion of topside ionograms with the profile-fitting method, *Radio Sci., 17,* 4, 837, 1982.

Jackson, J.E, E.R. Schmerling, and J.H. Whittacker, Mini-review on topside sounding, *IEEE Trans. Propag., AP 28(2),* 284,1980.

Khazanov, G. V., M. A. Koen, Y. V. Konikov, and I. M. Sidorov, Simulation of ionosphere-plasmasphere coupling taking into account ion inertia and temperature anisotropy, *Planet. Space Sci., 32,* 585, 1984

Lemaire J. and K. Gringauz, *The Earth's Plasmasphere*, with contributions from D.L. Carpenter and V. Bassolo, Cambridge Univ. Press, Cambridge, 346 pp., 1998.

Newberry, I. T., R. H. Comfort, P. G. Richard, and C. R. Chappell, Thermal He+ in the plasmasphere: Comparison of observations with numerical calculations, *J. Geophys. Res., 94,* 15,265, 1989.

Persoon, A. M., D. A. Gurnett, and S. D. Shawhan, Polar cap electron densities from DE 1 plasma wave observations, *J. Geophys. Res., 88,* 10,123, 1983.

Reinisch, B. W., G. S. Sales, D. M. Haines, S. F. Fung, W. W. L. Taylor, Radio wave active Doppler imaging of space plasma structures: Arrival angle, wave polarization, and Faraday rotation measurements with the radio plasma imager, *Radio Sci., 34,* 1513, 1999.

Reinisch, B.W. et al., The radio plasma imager investigation on the IMAGE spacecraft, *Space Sci, Rev., 91,* 319, 2000.

Reinisch, B.W. et al., First results from the radio plasma imager on IMAGE, *Geophys. Res. Lett., 28,* 1167, 2001.

Song, P., et al., Structure and Properties of the Subsolar Magnetopause for Northward IMF: Multiple Instrument Particle Observations, *J. Geophys. Res., 98,* 11319, 1993.

Song, P., and C. T. Russell, Time series data analyses in space physics, *Space Science Reviews, 87,* 387-463, 1999.

Tsyganenko, N.A. and D.P. Stern, Modeling the global magnetic field and the large-scale Birkeland current systems, *J. Geophys. Res., 101,* 27187-27198, 1996.

S. F. Fung and J. L. Green, NASA Goddard Space Flight Center, Code 630, Greenbelt, MD 20771.

D. Gallagher, NASA Marshall Space Flight Center, Space Science Department/ SD50, 320 Sparkman Drive, Huntsville, AL 35805.

X. Huang, B. W. Reinisch, G. S. Sales and P. Song, Environmental, Earth, and Atmospheric Sciences Department, Center for Atmospheric Research, University of Massachusetts, Lowell MA 01854 (email: Bodo_Reinisch@uml.edu).

V. M. Vasyliunas, Max-Planck-Institut fuer Aeronomie Max-Planck Str. 2, 37191 Katlenburg-Lindau, Germany.

(Received June 27, 2001; revised September 25, 2001; accepted October 25, 2001.)